Design and Implementation of a Two-Level Supervisory Fuzzy-PID Controller for Microjet Engine

Mohsen Shojaei[1], Mehdi Jahromi[2*], SayedHossein Sadati[3], Afshin Valimohammad[4]

Abstract–A detailed modeling of the thermodynamic behavior of the gas turbine engine has been developed in this study. The modeling encompasses volume dynamics, shaft dynamics, Mach number and altitude variation. To achieve maintaining of engine in desired operational range, a two-level hybrid fuzzy-PID controller has been designed for controlling a turbojet engine in a software environment. The effectiveness of this design approach has been investigated, considering all nonlinear thermodynamic behaviors and variations in Mach/altitude. The controller effectively manages these factors and have desire response. Furthermore, a protection loop has been implemented to safeguard against sudden engine shutdown, sharp temperature increases, and surge using the Min-Max strategy coupled with a controller. This approach ensures a safe response of the controller to the engine and prevents damage to the engine. The model possesses the capability to simulate the engine's performance in both transient and steady-state conditions. The validation of the thermodynamic model has been carried out using the Gas Turb 13 software to ensure acceptable simulation results. The maximum error was 7% in thrust level. The simulation results indicate the capability of the hybrid two-level controller in various flight scenarios, resulting in an average 18.6% shorter settling time, 34.3% shorter rise time, and no permanent error compared to PID control.

Keywords:Fuzzy controller,Gas turbine engine, Min-Max control strategy, Two-level controller

1. Introduction

The gas turbine engine, sometimes referred to as a combustion turbine, is widely used for power generation in aircraft, ships, trains, and power plants. It is predicted that in the coming decades, with advancements in manufacturing and design fields, gas turbines will play a more significant and prominent role in power generation across various industries.

Aerospace engines and gas turbines are generally known for their high operating temperatures, high speeds, and high pressures [1].

The control of aerospace engines and gas turbines is of great importance due to various performance and structural constraints, such as the rotational speed and acceleration of shafts, turbine inlet temperature, compressor surge margin, and so on [2,3].

In recent years, we have witnessed an increase in complexity in the design and performance of aerospace gas turbine engines in order to overcome current limitations and meet the requirements of new air routes set by governments and various organizations [4].

From a historical perspective, the design and development of jet engine controllers can be categorized into four main groups: 1. Hydro-mechanical fuel controllers, 2. Hydro-mechanical/electrical controllers, 3. Digital electronic controllers, and 4. Fully digital controllers [5].

However, the use of fuel flow in controlling the closed-loop speed and limiting fuel flow in transient regimes remains the primary strategy in jet engine controller design. As the engine design becomes more complex, the expectations and constraints that the controller must fulfill increase accordingly.

In recent years, more advanced and sophisticated algorithms have been employed in the control of gas turbine engines, including Model Predictive Control (MPC), Linear Quadratic Regulator (LQR), Linear Quadratic Gaussian (LQG) controller, and Fuzzy Logic controller.

Among these algorithms, fuzzy controller offers advantages such as similarity to human reasoning, linguistic modeling, the use of simple mathematics for complex problems, the ability to interact with integrated and complex systems, high accuracy and high responsiveness.

2* Corresponding Author: Faculty of Aerospace, Malek Ashtar University of Technology,Tehran, 1774-15875, Iran. Email:mjahromi@mut.ac.ir

1,3,4 Faculty of Aerospace, Malek Ashtar University of Technology,Tehran, 1774-15875, Iran.

Received:2024.06.06; Accepted: 2024.08.15

It also has its drawbacks such as the need for more fuzzy rules to achieve higher accuracy, the inability to use feedback for self-learning strategies, and limitations in utilizing input variables [6]. Fuzzy logic controller is a heuristic methodthat can easily use in designing of non-linear controllers.

Fuzzy controllers outperform other controllers in complex, non-linear systems or systems that are not well-defined [7]. Due to its simplicity and high reliability, PID controllers are widely used for controlling the performance of aerospace engines and gas turbines.

Common methods used to optimize PID controller coefficients in industries include the Cohen-Coon and Ziegler-Nichol's methods.

In these methods, it is assumed that the behavior of the system around the operating set point is linear. Based on this assumption and using the algorithms governing these methods, the values of the proportional gain (Kp), derivative gain (Kd), and integral time gain (Ki) are calculated to maintain the system's performance around the design points.

To achieve an appropriate response in systems that exhibit uncertainty and multiple complex and nonlinear relationships, PID controllers need to be continuously optimized. Therefore, in this research, a two-level fuzzy-PID supervisory system with its self-tuning algorithm is proposed for an integral-thermodynamic model of a turbojet engine.

Here are some of the notable achievements in the field of fuzzy controller design for gas turbine engines:

In 1994, Balakrishnan et al. proposed a set of fuzzy rules, laws, and logics for gas turbine control to provide an optimal and precise controller compared to conventional methods. They implemented this controller entirely based on fuzzy logic on a single-shaft gas turbine engine as a case study [8].

In 2002, Chipperfield et al. combined fuzzy logic with an evolutionary algorithm (EA) to optimize the controller's performance and enhance the system's maneuverability [9].

In 2023, Davoodi et al. conducted an HIL test for a fuzzy controller with min-max strategy for a non-linear model of a two-axis turbofan engine with high bypass. The results showed the controller's ability to generate the required thrust while adhering to structural and functional limitations [10].

In 2024, Zhimeng et al. successfully developed an accurate model of a three-axis gas turbine engine for ships and validated the model against actual test data. By optimizing the PID control coefficients using fuzzy rules, they were able to increase the power response from the model by approximately 3.1 times and prevent phenomena such as compressor surge and turbine overtemperature [11].

In 2015, Hadroug and colleagues utilized an adaptive neuro-fuzzy controller to maintain the system's performance in the optimal state. The results of the implemented controller on the Rowen model demonstrated the effectiveness of the proposed controller [12].

In 2018, Jafari and Nikolaidis improved the performance of the min-max strategy by replacing the maximum and minimum functions with different fuzzy norms and studied the advantages and disadvantages of each case [13].

In 2020, Guolian et al. introduced a fuzzy modeling approach, a disturbance rejection capability, and reduced settling time. They also presented a predictive control algorithm related to this model and implemented it on a gas turbine system [14].

During the activities and efforts carried out in the design and optimization of gas turbine controllers, the clear absence in using thermodynamic models that are highly accurate in simulating the dynamic behavior of the turbojet engine and also two-level controllers such as the fuzzy-PID two-level controller is evident; therefore, this research was conducted to take a step forward in this area.

.

2. Two-Level Non-Adaptive Fuzzy-PIDController

The common PID controllers tuned based on Ziegler-Nichols rules [15-17] for various gas turbine models have constant control gains. To have an optimized control system that dynamically adjusts control gains online during operations, we utilize a supervisory fuzzy-PID two-level controller.

In gas turbine models with complex structures, multi-level controllers operate much more efficiently than single-level controllers. In this two-level controller, at the lower level, the PID controller performs direct and quick model control, while the fuzzy controller at the higher level carries out system monitoring operations at a slower pace.

The main advantage of this control model, compared to single-level control, is the use of different simple controllers to enhance the overall system efficiency. For example, it is possible to design a fuzzy controller without considering stability issues and use another controller to monitor it.

As shown in Fig. 1, the error (e) and error rate (ė) are the inputs to the control system, and K_P, K_I, and K_D are respectively the proportional gain, integral gain, and derivative gain of the outputs of the fuzzy block.

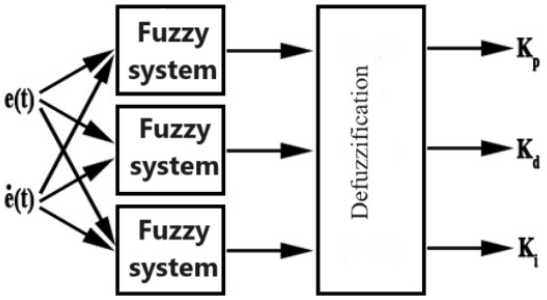

Fig. 1. Fuzzy system for tuning PID controller parameters [18]

For the input membership functions, simple triangular functions have been used (Fig. 2):

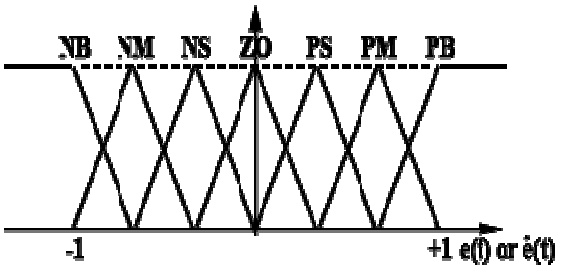

Fig. 2. Membership functions for inputs [18]

Where N represents negative and P positive. Also, S for small, M for medium, B for big, and ZO for zero; therefore, for example, NS signifies small negative error (error rate) and PB denotes big positive error. To prevent the defined fuzzy system from being specific to a particular system and for the sake of simplification, the coefficients are first normalized in the range [0, 1] as follows (Eqs. 1-2):

$$K_p{}' = \frac{K_p - K_{p_{min}}}{K_{p_{max}} - K_{p_{min}}} \quad (1)$$

$$K_d{}' = \frac{K_d - K_{d_{min}}}{K_{d_{max}} - K_{d_{min}}} \quad (2)$$

In Eqs. (1-2): $K_{d_{max}} = 0.15K_uT_u$, $K_{d_{min}} = 0.08K_uT_u$, $K_{p_{max}} = 0.6K_u$, $K_{p_{min}} = 0.32K_u$ [18],Where K_u is the ultimate gain resulting in oscillations at the stability boundary of the system with a proportional controller, and $T_u$is the period of these oscillations, These ratios are obtained through trial and error.

Now, if the ratio of two time constants is defined as $\alpha = T_i/T_d$, the third parameter can be written as Eq. 3:

$$K_i = \frac{{K_p}^2}{\alpha K_d} \quad (3)$$

Given that the fuzzy output sets $K_p{}'$and $K_d{}'$ are divided into two categories, big and small, their membership functions are as follows (Fig. 3):

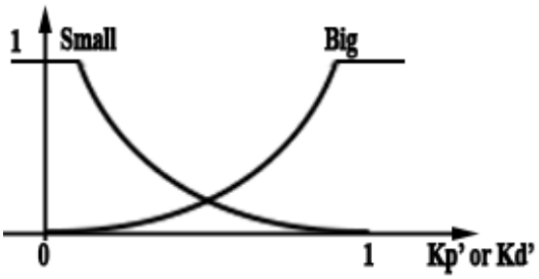

Fig. 3. Membership functions for $\acute{K}_P$and $\acute{K}_d$ [18]

Therefore, by having the system error and its rate as inputs, and the gains $\acute{K}_P$, $\acute{K}_d$, and α as outputs, a 2-input-1-output system can be designed for continuous and online updating of PID coefficients. The fuzzy rule table consists of 49 rules (seven rules for error and seven rules for error rate). Fuzzy rules are formulated using a set of if-then rules, for example:

If e is PB and $\dot{e}$ is ZO, then $K_p{}'$ is Big, $K_d{}'$ is Small and $\alpha = 2$.

In this manner, 49 rules are defined, and these rules are combined using the Mamdani fuzzy inference engine, singleton fuzzifier, and centroid defuzzifier [18]. Therefore, for online defuzzification of $\acute{K}_P$', $\acute{K}_d$, and α, we have (Eqs. 4-6):

$$K_p'(t) = \frac{\sum_{l=1}^{49} \bar{y}^l{}_p \mu_{A^l}(e(t))\mu_{B^l}(\dot{e}(t))}{\sum_{l=1}^{49} \mu_{A^l}(e(t))\mu_{B^l}(\dot{e}(t))} \quad (4)$$

$$K_d{}'(t) = \frac{\sum_{l=1}^{49} \bar{y}^l{}_d \mu_{A^l}(e(t))\mu_{B^l}(\dot{e}(t))}{\sum_{l=1}^{49} \mu_{A^l}(e(t))\mu_{B^l}(\dot{e}(t))} \quad (5)$$

$$\alpha(t) = \frac{\sum_{l=1}^{49} \bar{y}^l{}_\alpha \mu_{A^l}(e(t))\mu_{B^l}(\dot{e}(t))}{\sum_{l=1}^{49} \mu_{A^l}(e(t))\mu_{B^l}(\dot{e}(t))} \quad (6)$$

Where $A^l$and B^l are e and ė fuzzy sets respectively and $\bar{y}^l{}_p$,$\bar{y}^l{}_d$ and $\bar{y}^l{}_\alpha$ are fuzzy centers for $\acute{K}_P$, $\acute{K}_d$ and α respectively [18]

3. Engine Modeling

In the present research, in addition to the volume dynamics and rotor dynamics effects, the influence of humidity has also been considered to more accurately analyze the engine behavior at all flight points. The components of a single-shaft turbojet engine and the numbering of its parts are shown in the Fig. 4:

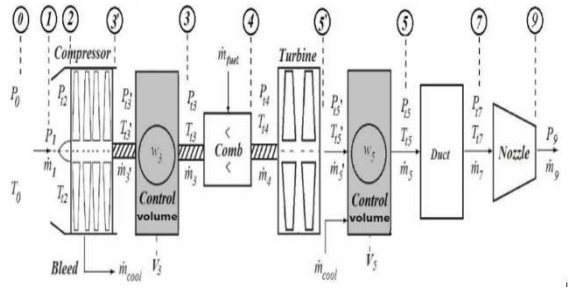

Fig. 4. Schematic of various sections of a turbojet engine

Each of the different sections of the turbojet engine has been modeled, including the air inlet, compressor, combustion chamber, turbine, and nozzle, as separate block diagrams developed in the Simulink environment based on the thermodynamic relationships governing each section in this model.

no linearization around the design point has been conducted, and the integral-thermodynamic model simulates the engine performance in the form of a set of nonlinear and interconnected equations. The modeling of the main engine parts includes the inlet, compressor as an integrated unit, combustion chamber, turbine as an integrated unit, and the outlet nozzle.

To model the engine behavior in transient regimes, the shaft dynamics are treated as an independent unit, along with volume dynamics represented by two control volumes in the model.The first control volume connects the compressor to the combustion chamber, while the second control volume links the turbine to the associated nozzle.

The mathematical and thermodynamic relationships derived for each section, as well as the modeling of shaft dynamics, volume dynamics, and humidity effects, are extracted from Ref. 19.

For modeling the transient regime of the engine, where performance parameters are changing over time, we utilize a combination of rotor dynamics and volume dynamics.

3.1 Rotor Dynamics

It is assumed that in a single-shaft turbojet engine operating in a steady state, the control system abruptly reduces the fuel flow, leading to a decrease in the temperature of combustion products and the output power of the turbine. This reduced power is less than the required power for the compressor, auxiliary equipment, etc.

Therefore, for transient conditions, an unbalanced power according to Eq. (7) is created. Numbering is based on Fig. 4.

$$\frac{dP_w}{dt} = \dot{m}_4.C_{P\,gas}.(T_4 - T_5) - \dot{m}_2.C_{P\,air}.(T_3 - T_2)/\eta_m \quad (7)$$

In the Eq. (7), $\eta_m$represents mechanical efficiency. This unbalanced power causes a deceleration on the shaft, and the trend of its changes is shown Eq. (8):

$$\frac{dN}{dt} = \left(\frac{60}{2\pi}\right)^2 \times \frac{1}{I \times N} \times \frac{dP_w}{dt} \quad (8)$$

In Eq. (8), N and I represent the rotational speed in rpm and the polar moment of inertia of the shaft in $Kg.m^2$, P_w is net power extracted from engine in Watt respectively. By using the Eq. 7 and Eq. 8, the rotational speed of the shaft can be calculated at any given moment.

These equations are placed in a separate block of shaft dynamics in the Simulink environment. During the acceleration operation, the unbalanced power is positive, leading to an increase in the overall speed.

2.2 Volume Dynamics

In transient regime is not valid to assume that pressure, temperature, and ultimately density remain constant as they change over time. This phenomenon, known as volumetric dynamics, can impact the transient performance of turbine sections, the combustion chamber, and the compressor.

Fig. 5 depicts the control volumes of a single-shaft turbojet engine. The first control volume connects the compressor to the combustion chamber, while the second control volume links the turbine to the associated nozzle.

Eq. 9 is used to calculate the mass accumulation rate in these two control volumes, respectively, to determine the rate of change in the output pressure from the compressor and turbine.

$$\frac{dW}{dt} = \dot{m}_{in} - \dot{m}_{out} \quad (9)$$

Where W is accumulatedmass, $\dot{m}_{in}$is inlet mass flow and $\dot{m}_{out}$ is oulet mass flow. Using the ideal gas equation, Eq. 9 can be rewritten as follows:

$$\frac{dP}{dt} = \frac{(\dot{m}_{in} - \dot{m}_{out})RT}{Vol} + \frac{P}{T}\frac{dT}{dt} \quad (10)$$

In Eq. 10, Vol represents the size of the control volume in m^3. By integrating the equation over the mentioned control volumes, one can calculate the output pressure of the

compressor and the turbine, respectively.

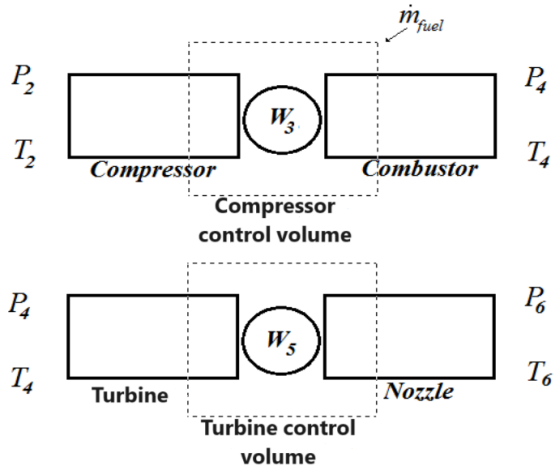

Fig. 5. Control volume for turbojet engine [20]

By examining the energy conservation (Eq. (11)) in each of these control volumes, one can calculate the rate of temperature change from Eq. (11).

$$\frac{dU}{dt} = (\dot{m}C_PT)_{in} - (\dot{m}C_PT)_{out} + Q_{out} \tag{11}$$

In Eq. 11, $U = W * u$ and $u = C_v * T$By simplification, we get:

$$\frac{dT}{dt} = \frac{(\dot{m}C_PT)_{in} - (\dot{m}C_PT)_{out} + Q_{out}}{W.C_v} + \frac{T}{W}\Delta\dot{m} \tag{12}$$

In Eqs. 11-12, the term Q refers to the heat transfer between engine components and the adjacent fluid.
All of these calculations have been implemented in Simulink. Finally, the engine has been modeled in Simulink as Fig. 6 and Fig. 7.

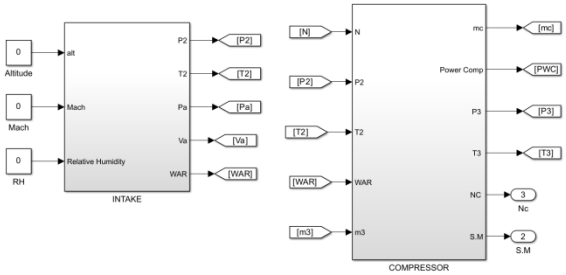

Fig. 6. An image of the final model in Simulink part 1

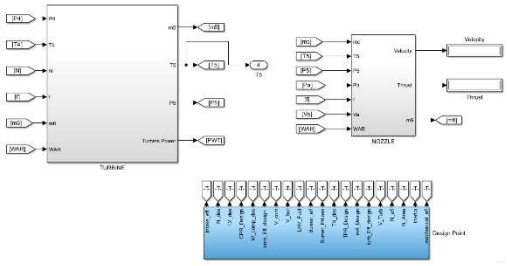

Fig. 7. An image of the final model in Simulink part 2

4. Model Validation

Modeling the engine components based on design point variables has the advantage that by changing the performance curves of the compressor and turbine, as well as the design point specifications, the performance of another single-shaft turbojet engine can be simulated. Table 1 shows the specifications of the design point for the BMT-KS120 microjet engine.

Table 1.BMT-KS120 specifications at design point

Parameter	Value
Inlet mass flow rate	0.288 Kg/s
Compressor pressure ratio	3.15
Exhaust temperature	985 K
Mechanical efficiency	0.98
Compressor efficiency	0.816
Combustion chamber efficiency	0.9
Turbine efficiency	0.85
Shaft inertia mass	0.0001179 $Kg.m^4$
Rotational speed at design point	120000 rpm

For validation of the results of the developed model, one of the most popular gas turbine modeling software called Gasturb 13 is used. With Gasturb 13 software, the transient performance and steady-state configurations of various gas turbines can be simulated.
For transient validation, a two-stage maneuver in twenty seconds is considered. Three speeds are
selected for this maneuver: corrected speed of 0.7 design point speed, back to speed one, and again to speed one. The slope of these maneuvers is set to 2.5 seconds to prevent any sudden temperature spikes and approaching too close to surge margins.
Fuel flow equivalent to these speeds is provided as input, and its data is compared with the Gasturb model. The ODE-

45 solver is used to solve the equations, which, in comparison with other solvers, provides a suitable level of accuracy with variable time steps.

The tolerance of 10^{-7} has been determined as the calculated response tolerance. The rotational speed and thrust level for both simulations and the error of the developed model are shown in Fig. 8 and Fig. 9 The maximum error of the current model compared to the Gasturb 13 model is 1.32% for rotational speed and 7% for thrust level.

The results indicate that the current model is sufficiently accurate in predicting the transient behavior of the engine.

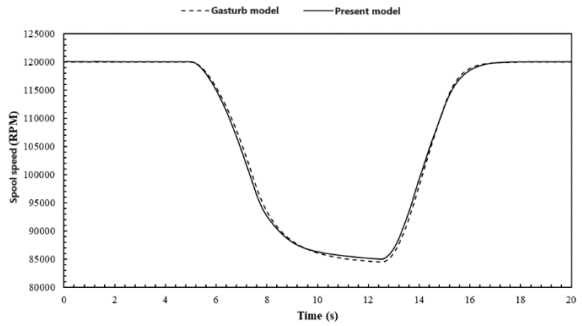

Fig. 8. Comparison of engine speed in the present model with Gasturb 13 software.

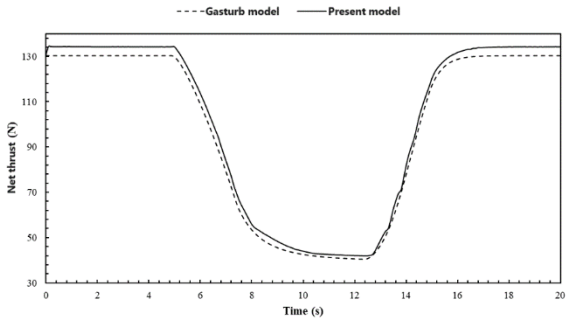

Fig. 9. Comparison of thrust in the present model with Gasturb 13 software model

5. Min-Max Strategy

The control system of an aircraft engine must satisfy all control modes simultaneously. These modes include steady-state control mode, transient control mode, and physical limiters control mode.

The steady-state mode is responsible for tracking and executing input commands to the system with the least error. The transient mode is responsible for meeting thrust requirements in the shortest possible time, and the physical limiters mode must protect the engine from reaching physical limits such as overspeed, combustion chamber shutdown, stall, exceeding permissible turbine inlet temperature, etc.

All of these control modes must be satisfied simultaneously to ensure precise performance and safety of the engine. Since 1952, several methods for implementing control systems for aircraft engines and gas turbines have been proposed, each with its own advantages and disadvantages.

A comprehensive comparison of various strategies for controlling aircraft engine systems has been conducted in Refs. [2 , 20]. The Min-Max strategy has been recognized for years as a practical method capable of satisfying all control modes. A min-max controller consists of several control loops[21 - 22]

- A steady-state control (PLA) that calculates the fuel flow for steady-state conditions based on engine operational conditions.
- An Acceleration and Deceleration Control Loop that controls the acceleration and deceleration phases based on input commands to the control system.
- A physical limitations control that ensures requirements based on physical limitations such as combustion chamber shutdown, maximum shaft speed, maximum turbine inlet temperature, etch

The general structure of min-max control is depicted in Fig. 10. As shown in the Fig. 10, the fuel flow entering the system can be divided into two parts: the first part is the fuel flow calculated by the steady-state control mode, and the second part is the fuel flow determined by the transient control mode or physical limitations.

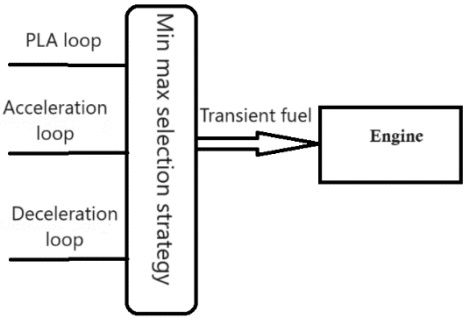

Fig. 10. Schematic of the min-max control loop in a turbojet engine

In order to choose the best control loop for calculating fuel flow in transient mode, the structure of the min-max strategy is rewritten in the form of Eq. 13.

$$W_{ftr} = Max\left(Min\left(W_{fPLA}, W_{facc}\right), W_{fdec}\right) \quad (13)$$

Where W_{ftr} is transient control loop's fuel mass flow signal, W_{fPLA} is PLA control loop's fuel mass flow singal,

W_{facc} is acceleration control loop's fuel mass flow signal and W_{fdec} is deceleration control loop's fuel mass flow signal.

6. Closed-Loop System Simulation

Next, we move on to implementing the controller on the BMT-KS120 engine model, which has been modeled as described in Modeling Section.
In the next step, we consider three different scenarios for the transient mode in the engine to evaluate the performance of the control system. This scenario without the control system will be compared with the control system.

6.1. Case study 1: transient regime without controller unit

The engine configuration in this case study is an open-loop system, as no control subsystem is utilized, and the main goal is to investigate the behaviors of engine parameters in transient mode. In this case study, the fuel mass flow rate shown in Fig. 11 for the engine at sea level and Mach 0 is applied to the system from the steady-state regime to obtain the idle point value for 20 seconds.
From this moment onwards, the mass flow rate increases in a step command manner up to 1.43 times the idle point value to achieve the take-off speed. The mass flow rate command remains at this level for 20 seconds and then returns to its initial value with another step command.

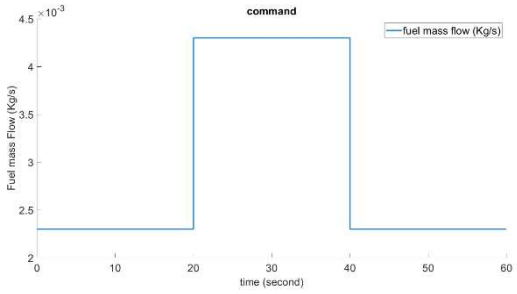

Fig. 11. Applied fuel flow ($\frac{Kg}{s}$) to the BMT-KS120 model for simulating transient mode without a controller.

This step command covers a wide range of the compressor performance map and may potentially lead the engine beyond its operational limits. Evaluating the engine performance due to the step command without a control system provides a good insight into the reasons for using limiters and designing a control system.
Furthermore, in Figs. 12-13, Turbine inlet temperature variation and Surge margin variation can be seen respectively.

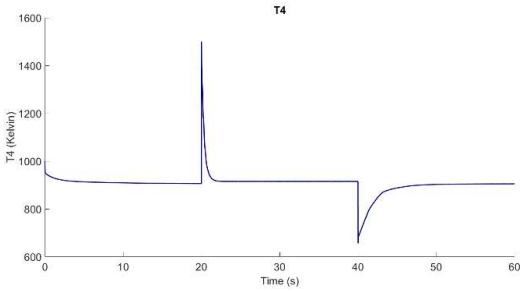

Fig. 12. Turbine inlet temperature variation at sea level without a controller

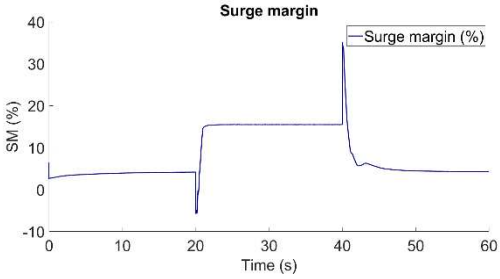

Fig. 13. Surge margin variation at sea level without a controller

To achieve the goal of having a safe operation, a simple and practical approach has been employed to limit the engine parameters' reactions to sudden maneuvers in transient mode. During sudden increases or decreases in shaft speed, the engine may be susceptible to phenomena such as surge or combustion chamber flame-out.
As evident from Fig. 12 and Fig. 13, sudden temperature changes due to abrupt fuel command variations and the surge margin approaching a critical range can lead to catastrophic consequences for the engine, surpassing the operational envelope.
Analyzing these maneuvers on the compressor map reveals that a decrease in speed maneuver causes the performance to approach the lower limit of the operational range, while an increase in speed maneuver brings the performance close to or even beyond the upper limit of the operational envelope.
Since the controlled parameter in this study is the fuel flow rate, a common method is to plot the modified fuel flow rate equation $\dot{m}_f$ / [(P_2/P_{2ref}) $(\dot{m}_{fmax}\sqrt{T_2/T_{2ref}})$] relative to the corrected rotational speed $N/(N_{max}\sqrt{T2/T1ref})$, which provides the operational envelope.
In the above equations, N_{max} represents the take-off

rotational speed and $\dot{m}_{fmax}$ denotes the fuel flow rate for achieving take-off speed. For safe flight, the engine fuel flow rate must be controlled in a way that it always falls within the operational envelope.

6.2. Case study 2; Transient Regime withControl Unit

The aim of this case study is to investigate the impact of the control system on the engine behavior in transient mode. You can see the overall closed-loop system in Fig. 14.

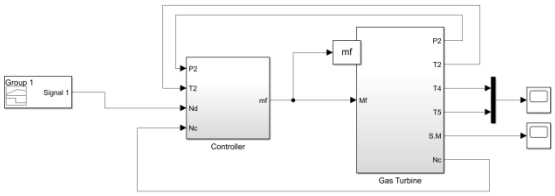

Fig. 14. Thermodynamic model of a turbojet engine with feedback control.

This control system, as described earlier, consists of three control loops: the steady-state control mode, which is a two-level hybrid fuzzy-PID supervisory control. The acceleration control mode and the deceleration control mode, discussed in case study number two.

When the pilot command is applied to the system, the closed-loop control system, using feedback from the modified rotational speed, calculates the required fuel flow rate to achieve the command.

The steady-state control mode issues a command using a mechanism described in the strategy determination section, while the acceleration control mode and deceleration control mode suggest their mass flow rate based on a table graph implemented in the Simulink environment and receiving feedback of the modified rotational speed.

Finally, based on the strategy outlined in the Min-Max strategy, the fuel flow control system issues a mass flow rate command to the system. In the following, we will examine three case studies at various altitudes and Mach numbers to assess the impact of the control system on each other.

The selected scenario for each case is the worst-case scenario, involving sudden changes (rapid increase and decrease in speed) on a very large scale (from idle to take-off), and as a result, the performance of the control system against this scenario is evaluated.

6.2.1 Scenario 1: Mach 0 Altitude 0 Meter

Based on the information obtained from the validated model, the modified idle speed is equal to 0.7. In the first case study, considering an altitude controller of 0 and a Mach number of 0, we start from idle speed for 20 seconds to take-off speed using a command.

The command remains at take-off speed for 20 seconds until the 30th second. Then, the command returns to idle speed. The simulation duration is 60 seconds.

The transient characteristics of the two-level hybrid fuzzy-PID controller in this scenario are summarized in Table 2.

Table 2. Transient characteristics of the fuzzy-PID controller in the first scenario

Parameter	Value	Unit
Rise time	2.71	S
Settling time	3.16	S
Overshoot	0	%

The plots related to the system input command and system response, turbine inlet temperature and margin of safety can be observed in Figs. 15-17respectively.

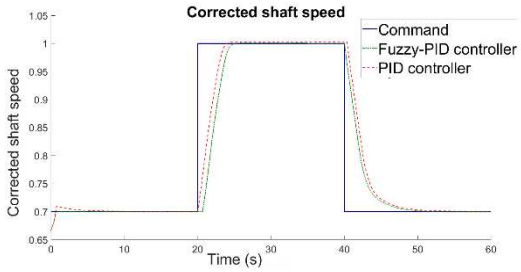

Fig. 15. Plot of corrected shaft speed and command in the first scenario

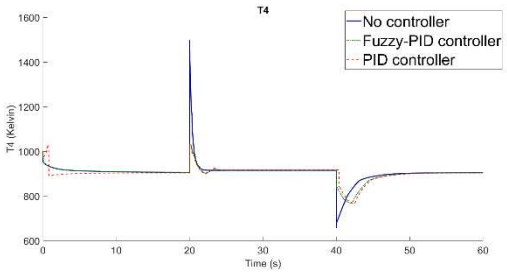

Fig. 16. Turbine inlet temperature in the first scenario

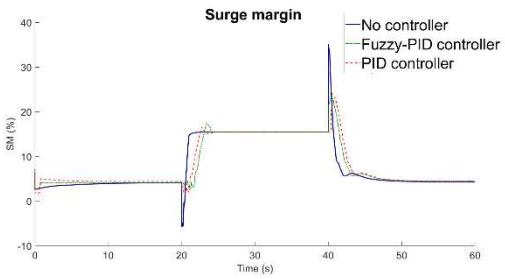

Fig. 17. Plot of surge margin in the first scenario

As evident from the plot in Fig. 16, the control system prevents sudden jumps in turbine inlet during acceleration and deceleration, thereby avoiding phenomena such as combustion chamber flameout and turbine blade damage.

On the other hand, due to the stiffening process of increasing compressor outlet pressure and consequently the gradual increase in negative pressure gradient, the safety margin at the surge limit during acceleration (Fig. 17) remains within the 5% range, which is a standard value for transient regimes [2].

A summary of the performance parameters in the presence and absence of the control system is provided in Table 3 Another advantage of the control system is the elimination of undershoot and reducing the temperature rise in the engine's hot section from the idle temperature. This ensures the prevention of combustion chamber flameout incidents.

Table 3. Comparison of thermodynamic and performance parameters in two conditions: without controller and with controller in the first scenario

Parameter	Unit	Without controller	Fuzzy-PID	PID
Minimum surge margin	%	-5.55	4.46	4.41
Maximum turbine Inlet temperature	K	1500.6	1030.01	1030.9
Turbine Inlet temperature overshoot	%	63.9	12.5	12.6

6.2.2 Scenario 2: Mach 0.4Altitude 2500Meter

The purpose of this case study and the following case study is to investigate the performance of the control system at different altitudes and Mach numbers. As mentioned in the modeling section, the integral-thermodynamic model allows simulating the effects of altitude.

In this new altitude, similar to the previous case study, we consider the worst-case scenario and a command from idle to take-off.

Using a command, we start from idle shaft speed for 20 seconds to take-off speed and then the command remains at take-off speed for 20 seconds until the 40th second.

The command then returns to idle speed. The simulation duration is 60 seconds. The transient characteristics of the control system in this scenario are summarized in Table 4.

Table 4. Transient characteristics of the fuzzy-PID controller in the second scenario

Parameter	Value	Unit
Rise time	1.28	S
Settling time	1.65	S
Overshoot	0	%

The plots related to the system input command and system response, turbine inlet temperature and margin of safety turbine inlet temperature can be observed in Figs. 18-20 respectively.

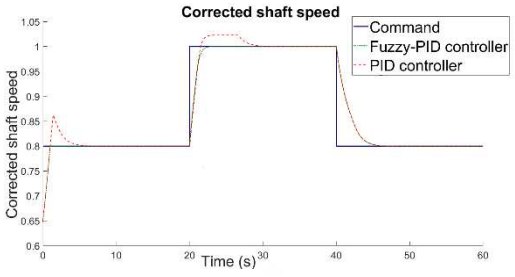

Fig. 18. Plot of corrected shaft speed and command in the second scenario

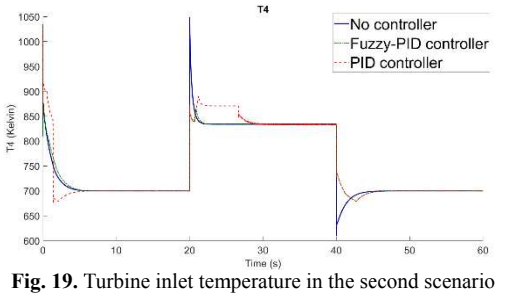

Fig. 19. Turbine inlet temperature in the second scenario

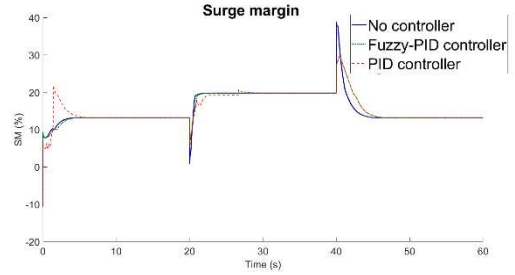

Fig. 20. Plot of surge margin in the second scenario

Similar to the previous case study, in Figs. 18- 20, it can be observed that the control system successfully achieves its main objectives of having a fast response with minimal error (Fig. 18), preventing the engine's hot section temperature from entering the danger zone and avoiding combustion chamber flameout (Fig. 19) and maintaining a safety margin within the 5% limit in transient regimes (Fig. 20).

A summary of the behavior of the engine's thermodynamic parameters in the presence and absence of the control system is provided in Table 5.

Table 5. Comparison of thermodynamic and performance parameters in two conditions: without controller and with controller in the second scenario

Parameter	Unit	Without controller	Fuzzy-PID	PID
Minimum surge margin	%	0.84	6.03	5.89
Maximum turbine inlet temperature	K	1049	864.9	890.3
Turbine inlet temperature overshoot	%	25.8	3.7	6.77

6.2.3 Scenario 3: Mach 0.6Altitude 5000Meter

In the latest case study, similar to the two previous studies, we simulate the worst-case scenario with a command for 60 seconds starting from the corrected idle speed (0.85) to take-off speed and then returning to idle speed.The transient characteristics of the control system are summarized in Table 6.

Table 6. Transient characteristics of the fuzzy-PID controller in the third scenario

Parameter	Value	Unit
Rise time	0.83	S
Settling time	1.15	S
Overshoot	0	%

The plots related to the system input command and system response, turbine inlet temperature andmargin of safety can be observed in Figs. 21-23respectively.

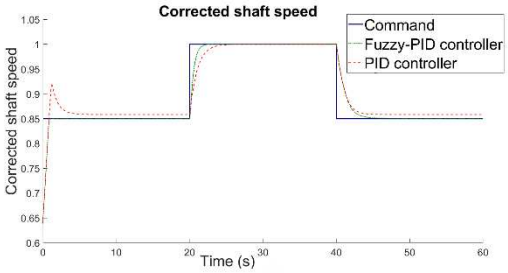

Fig. 21. Plot of corrected shaft speed and command in the third scenario

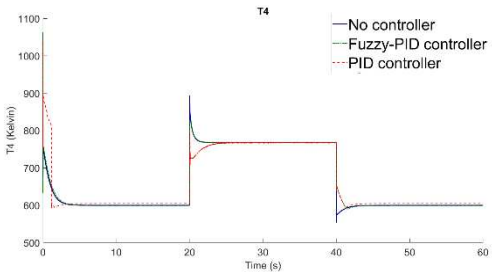

Fig. 22. Turbine inlet temperature in the third scenario

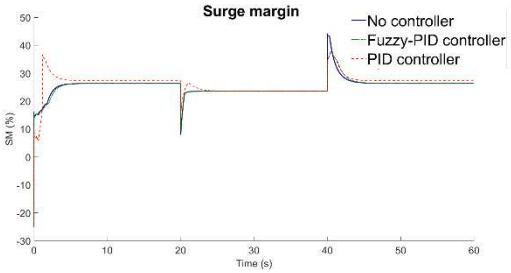

Fig. 23. Plot of surge margin in the third scenario

As evident from Figs. 21- 23, in this scenario, the control system successfully achieves its main objectives of having a fast response with minimal error (Fig. 21). the primary objective of the control system to keep the engine within safe operational limits and prevent occurrences such as turbine inlet temperature (Fig. 22) surge (Fig. 23) and exceeding acceptable limits is successfully achieved.
Its advantage is clearly highlighted compared to a system without a controller.A summary of the control parameters' behavior in this scenario, both with the controller and without the controller, is provided in Table 7.

Table 7. Comparison of thermodynamic and performance parameters in two conditions: without controller and with controller in the third scenario

Parameter	Unit	Without Controller	Fuzzy-PID	PID
Minimum surge margin	%	7.96	8.31	11.18
Maximum turbine inlet temperature	K	893.6	828.5	811.5
Turbine inlet temperature overshoot	%	15.844	7.400	5.199

7. Conclusion

In this research in order to demonstrate the impact of nonlinear relationships on engine behavior, an integral thermodynamic model was developed. The developed model was implemented in the Matlab/Simulink environment. For the sake of simplicity and faster computation speed, some researches in field of designing control system for air-breathing engines [10-14]In the initial phase of research have been done by linearizing and simplifying the equations governing the engine. In aforementioned researches conventional models such as the Rowen model or linearized transfer function models around design point are used, which cannot accurately simulate the transient behavior of the engine. By analyzing the results obtained from the present model and comparing and validating it with the model implemented in the reputable software Gasturb 13, the credibility and reliability of the

present model were established. Studying of engine and its behavior in steady-state and transient regimes clearly demonstrate the need for using a control system. In addition to that the quality of performance of the two-level hybrid controller is also demonstrated. In previous researches in this field [4, 13], credibility of pure fuzzy controller coupled with min-max strategy was proven with model in the loop approach and this research shows reliability of min-max strategy with hybrid fuzzy-PID controller. A comparison between pure fuzzy controller response [13] and hybrid fuzzy-PID controller is demonstrated in Table 8.

Table 8. Comparison of rise time and settling time

Author	Type of data	Type of controller	Mean rise time (s)	Mean settling time (s)
Present work	Numerical	Fuzzy-PID	1.6	1.98
Data [13]	Numerical	Pure fuzzy	2.71	3.2

In the transient regime studies, the worst-case scenario was considered for three different altitudes to precisely evaluate the performance of the control system. In all three cases, the hybrid supervisory fuzzy-PID controller successfully provided acceptable transient parameter responses.
It also maintained surge margin within a logical range for both transient and steady-state conditions, reduced temperature spikes in the hot section of the engine to prevent turbine blade damage during acceleration, andeliminated negative temperature spikes to prevent flameout.
Table 9andTable 10 summarize performance of two controllers in three case studies:

Table 9. Fuzzy – PIDcontroller performance in 3 case studies

Case study	Rise time (s)	Settling time (s)	Overshoot (%)
1	2.71	3.16	0
2	1.28	1.65	0
3	0.83	1.15	0

Table 10. PIDcontroller performance in 3 case studies

Case study	Rise time (s)	Settling time (s)	Overshoot (%)
1	2.7	3.16	0.197
2	1.13	1.36	2.28
3	2.208	2.98	0

As it is evident from Tables 9-10 and figures presented in case studies, the main advantages of the two-level controller compared to the PID controller include:

- No permanent error when reaching idle and take-off rotational speed.
- Elimination of any overshoot and undershoot during response convergence.
- The system control response being close to the physical reality governing the engine.

References

[1] St. Sergui, F. loana, P. Victor and S. Calin, "Gas Turbine Modelling Load Frequency Control", *UP.B. Sci. Bull, Series C*, Vol. 70, No. 4, pp. 13-20, (2008).

[2] L.C. Jaw, and J.D. Mattingly, "Aircraft Engine Controls: Design, System Analysis, and Health Monitoring", American Institute of Aeronautics and Astronautics, Reston, pp. 119-170, (2009).

[3] A. Linke-Diesinger, "Systems of Commercial Turbofan Engines: An Introduction to Systems Functions", Springer Science & Business Media, Berlin, pp. 85-99, (2008).

[4] S.J. Mohammadi Doulabi Fard, S. Jafari, "Fuzzy Controller Structures Investigation for Future Gas Turbine Aero-Engines", *Int. J. Turbomach. Propuls. Power*, Vol. 6, No. 1, pp. 2-24, (2021).

[5] J. Lutambo, J. Wang, Yue, H. Dimirovsky, "G. Aircraft turbine engine control systems development: Historical Perspective", *IEEE*, Vol. 34, No. 7260534, pp. 5736-5741, (2015).

[6] K. Michels, F. Klawonn, R. Kruse, A. Nürnberger, "Fuzzy Control", Springer, Berlin/Heidelberg, pp. 235-256, (2006).

[7] J. F. Silva, S.F. Pinto, "Power Electronics Handbook" , 4th ed., Academic press, San Diego, pp. 1141–1220, (2018).

[8] S.R. Balakrishnan, S.K. Mishra, V. Sundararajan, K.A. Damodaran, "Fuzzy Computing for Control of Aero Gas Turbine Engines", *Def. Sci. J.*, Vol. 44, No.4, pp. 295–304, (1994).

[9] A.J. Chipperfield, B. Bica, P.J. Fleming, "Fuzzy scheduling control of a gas turbine aero-engine: A

multiobjective approach", *IEEE Trans. Ind. Electron*, Vol. 49, No. 3, pp. 536–548, (2002).

[10] M. Davoodi, H. Bevrani, "A new application of the hardware in the loop test of the min–max controller for turbofan engine fuel control." *Adv. Control Appl.: Eng. and Ind. Syst.*, Vol. 5, No. 2, pp. 138-154, (2023).

[11] L. Zhimeng, Y. Liu, Youhong Yu, R. Yang, "Advanced fuel limit design to improve dynamic performance of marine three-shaft gas turbine." *Appl. Therm. Eng*, Vol. 236, No. 1, pp. 121-149, (2024).

[12] N. Hadroug, A. Hafaifa, M. Guemana, A. Kouzou, A. Salam, A. Chaibet, "Heavy duty gas turbine monitoring based on adaptive neuro-fuzzy inference system: Speed and exhaust temperature control", *MICS*, Vol. 8, No. 8, pp. 1-20, (2017).

[13] S. Jafari, T. Nikolaidis, "Turbojet engine industrial min-max controller performance improvement using fuzzy norms", *Electronics*, Vol. 4, No. 11, pp 314-337, (2018).

[14] H. Guolian, G. Linjuan, H. Congzhi, Z. Jianhua, " Fuzzy modeling and fast model predictive control of gas turbine system", *Energy*, Vol. 200, No. 1, pp. 117-165, (2020).

[15] J. G. Ziegler, N. B. Nichols, "Optimum setting for auto-matic controllers", *Trans. ASME*, Vol. 64, No. 8, pp. 759-765, (1942).

[16] A. S. McCormack, K.R. Godfrey, "Rule-based autotuning based on frequency domain identification", *IEEE Trans. Control Syst. Technol*., Vol. 6, No. 1, pp. 43–61, (1998).

[17] D. W. Pessen, "A new look at PID-controller tuning", *J. Dyn. Syst. Meas. Control*, Vol. 116, No.1, pp. 553–557, (1994).

[18] Z. Y. Zhao, et al, "Fuzzy Gain Scheduling of PID Controllers", *IEEE Trans. Syst. Man Cybern*., Vol. 23, No. 5, pp. 1392-1398, (1993).

[19] P. P. Walsh, P. Fletcher, "Gas Turbine Performance", 2nd ed., Wiley, New York, pp. 61-101, (2004).

[20] A. Kreiner, K. Lietzau, "The Use of Onboard Real-Time Models for Jet Engine Control", *MTU Aero Eng.*, pp. 1-26, (2002).

[21] H.A. Spang III, H. Brown, " Control of jet engines", *Control Eng. Pract.*, Vol. 7, No. 9, pp. 1043-1059, (1999).

[22] I. Moir, A. Seabridge, "Engine Control Systems", Wiley, New York, pp. 51-86, (2008).